

Hopping conduction in strong electric fields: Negative differential conductivity

A. V. Nenashev,^{1, 2, *} F. Jansson,^{3, 4} S. D. Baranovskii,⁵ R. Österbacka,⁴ A. V. Dvurechenskii,^{1, 2} and F. Gebhard⁵

¹*Institute of Semiconductor Physics, 630090 Novosibirsk, Russia*

²*Novosibirsk State University, 630090 Novosibirsk, Russia*

³*Graduate School of Materials Research, Åbo Akademi University, 20500 Turku, Finland*

⁴*Department of Physics and Center for Functional Materials, Åbo Akademi University, 20500 Turku, Finland*

⁵*Department of Physics and Material Sciences Center, Philipps-University, 35032 Marburg, Germany*

(Dated: September 23, 2008)

Effects of strong electric fields on hopping conductivity are studied theoretically. Monte-Carlo computer simulations show that the analytical theory of Nguyen and Shklovskii [Solid State Commun. 38, 99 (1981)] provides an accurate description of hopping transport in the limit of very high electric fields and low concentrations of charge carriers as compared to the concentration of localization sites and also at the relative concentration of carriers equal to 0.5. At intermediate concentrations of carriers between 0.1 and 0.5 computer simulations evidence essential deviations from the results of the existing analytical theories.

The theory of Nguyen and Shklovskii also predicts a negative differential hopping conductivity at high electric fields. Our numerical calculations confirm this prediction qualitatively. However the field dependence of the drift velocity of charge carriers obtained numerically differs essentially from the one predicted so far. Analytical theory is further developed so that its agreement with numerical results is essentially improved.

PACS numbers: 72.20.Ht, 72.20.Ee, 72.80.Ng, 72.80.Le

I. INTRODUCTION

Hopping conduction in solids governed by strong electric fields is in the focus of intensive theoretical and experimental study since several decades [see, for instance, chapter 7 in Ref. 1 and references therein]. In recent years, particular interest to this research area has been caused by growing device applications of amorphous organic and inorganic materials in which the incoherent hopping transitions of charge carriers between spatially and energetically distributed localized states dominate the optoelectronic phenomena [see, for instance, Ref. 2 and references therein]. One of the mostly discussed topics is whether the differential negative conductivity (NDC), i.e., the decreasing conductivity with increasing electric field, is possible in the hopping regime. The discussion was, to much extent, provoked by the reports on the apparent decrease of the drift mobility with rising electric field at relatively high temperatures and low field strengths in disordered organic materials.^{3,4,5,6,7,8,9,10} This apparent decrease of the mobility with increasing electric field was reported to be succeeded by the increase of the mobility at higher field strengths. However, the self-consistent effective-medium theory for drift and diffusion at low electric fields¹¹ does not show any decrease of the mobility with increasing field. Furthermore, it has been shown experimentally¹² and theoretically¹³ that the apparent decrease of the mobility with rising field at low field strengths is an artifact. The experimental data were obtained by the time-of-flight technique, in which charge carriers are created close to one surface of a sample with a given thickness L and the transient time τ_{tr} is measured, which is needed for charge carriers to reach the opposite

surface of the sample at a particular strength of the applied electric field F . Then the drift mobility is calculated as $\mu = L/(\tau_{\text{tr}}F)$. However, at high temperatures and low electric fields the current transients in the time-of-flight experiments are determined mostly by diffusion of charge carriers rather than by their drift. Therefore, using the drift formula one strongly overestimates the mobility. It is the presence of the field strength in the denominator that leads to the apparent “increase” of the mobility at decreasing F .^{12,13} If one uses at low fields and high temperatures the diffusion formulas instead of the drift ones, then no decrease of the mobility with increasing field can be claimed at low electric fields.^{12,13}

This result does not exclude, however, the possibility of the NDC in the hopping regime. Böttger and Bryksin¹⁴ and Shklovskii et al.^{15,16} have suggested analytical theories for the mobility and conductivity decreasing with increasing electric field in various disordered materials. Remarkably, this effect of the negative differential conductivity is to be expected at high field strengths. This regime succeeds the very strong increase of the mobility with rising field,^{15,16} and does not precede it at lower fields as claimed on the basis of the drift equations.^{3,4,5,6,7,8,9,10}

The decreasing conductivity with increasing electric field at high field strengths has been observed experimentally for hopping transport in lightly doped and weakly compensated crystalline silicon.^{17,18,19} The hopping transport mode in such systems at low electric fields had been described theoretically in all detail,²⁰ which made these systems particularly attractive for studying the new non-Ohmic effects. Shklovskii et al.^{15,17,18,19} developed an analytical theory, which predicted the NDC

effect in the lightly doped weakly compensated semiconductors. The experimental observations in lightly doped and weakly compensated crystalline silicon appear in qualitative agreement with his theoretical predictions. Furthermore computer simulations of Levin et al.²¹ confirmed qualitatively the existence of the NDC effect, though no quantitative comparison with the analytical theory¹⁵ has been attempted. Recent interest in the NDC effect has been caused by its importance for construction of memory devices. These devices typically contain conducting particles embedded into a nonconductive material. For such devices, made from both inorganic^{22,23} and organic^{24,25,26,27,28} materials, NDC and switching phenomena have been reported. Since electrical conduction in the materials, which are currently being tried for device applications, is dominated by hopping of charge carriers, it is necessary to study the possibility of the NDC in this regime in more detail.

In the present paper we report on the theoretical study of hopping transport in high electric fields. In Section II we describe the theoretical model and briefly outline the analytical approach suggested by Nguyen and Shklovskii¹⁵ for the limit of extremely high electric fields. In Section III we present our results obtained by straightforward Monte Carlo computer simulations and show the range of applicability for the analytical theory of Nguyen and Shklovskii. In Section IV we further develop the analytical theory whereby we improve its agreement with the results of computer simulations. In particular, the analytical dependence of the drift mobility on the concentration of charge carriers comes in better agreement with the simulation results. Section V is dedicated to the NDC. A new numerical algorithm has been developed to study the NDC effect theoretically. Numerical results obtained in the framework of this algorithm confirm qualitatively the conclusion of Nguyen and Shklovskii on the possibility of the NDC in the hopping regime. However, the field dependence of the drift velocity of charge carriers obtained numerically differs essentially from the one predicted so far.¹⁵ We suggest in Section V a further development of the analytical theory, improving essentially its agreement with numerical results. Concluding remarks are gathered in Section VI.

II. MODEL AND THEORETICAL BACKGROUND

Aiming to clarify whether the NDC effect is inherent for the hopping transport regime, we consider first, following Nguyen and Shklovskii,¹⁵ the simplest possible model—a three-dimensional array of isoenergetic sites with a random spatial distribution with the concentration N . Each site can be either empty or occupied by a single electron. Energies of electrons are equal on all sites so that no energy disorder and no electron-electron interactions between different sites are taken into account. Only in the final part of Section V we study the ef-

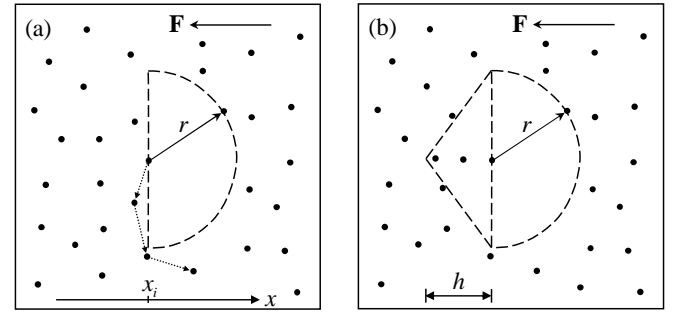


FIG. 1: The shape of optimal traps for the infinite (a) and a finite (b) electric fields. The dotted path in (a) is forbidden at infinite fields but provides an escape route at finite fields

fect of the energy disorder on the NDC. An electric field $\mathbf{F} = (-F, 0, 0)$ is put along the negative direction of the axis X , so that the drift velocity of the negatively charged electrons is directed along the X axis. Conduction takes place due to tunnelling hops of electrons between the localization sites. The rate Γ_{ij} for an electron hop from site i to site j is determined as

$$\Gamma_{ij} = \Gamma_0 \exp\left(-\frac{2d_{ij}}{a}\right) f\left(\frac{eF(x_j - x_i)}{kT}\right) n_i(1 - n_j), \quad (1)$$

where d_{ij} is the distance between the sites, a is the localization length, e is the elementary charge, k is the Boltzmann constant, T is the temperature, and n_i, n_j are the occupation factors of the sites, ($n_i, n_j \in \{0; 1\}$). The function f is related to energy the gain or the energy loss during the jump:

$$f(\alpha) = \begin{cases} 1, & \text{if } \alpha > 0, \\ \exp(\alpha), & \text{if } \alpha < 0. \end{cases}$$

In the limit of infinite electric field, the factor $f[eF(x_j - x_i)/kT]$ reduces to the Heaviside's function $\theta(x_j - x_i)$.

Below we will assume that $\Gamma_0 = e = 1$. As a measure of length, we introduce the typical distance between the neighboring sites $R = N^{-1/3}$.

Using this simple model, Nguyen and Shklovskii¹⁵ have shown analytically that the effect of the NDC is inherent for hopping transport. Let us consider briefly their arguments starting from the case of infinitely high fields F and extremely small electron concentrations n_e . Under such circumstances each electron can be treated independently from the others and electrons can move only toward the increasing values of their x coordinate. In Fig. 1 this is the direction to the right. At each jump, an electron moves along the axis X to a distance $\simeq R$, so that its drift velocity can be estimated as $v \simeq R/\tau$, where τ is an average time between jumps (dwell time). A dwell time τ_i for hopping from the site i is of the order of $\exp(2r_i/a)$, where r_i is the distance from site i to its nearest neighbor “to the right”, i.e. with co-ordinate x larger than x_i . In other words, r_i is the maximum

radius of a hemisphere centered at the site i that does not contain any other sites (Fig. 1(a)). If r_i is much larger than R (the typical distance between the neighboring sites), such an empty hemisphere can be considered as a trap for electrons. The contribution of traps with radii in the range $[r, r + dr]$ to the average dwell time $\bar{\tau}$ is proportional to $\tau(r) = \exp(2r/a)$, and also to the probability of the corresponding configuration of sites, $p(r)dr = 2\pi Nr^2 \exp(-2\pi Nr^3/3)dr$:

$$\bar{\tau} = \int_0^\infty \tau(r)p(r)dr = \int_0^\infty 2\pi Nr^2 \exp\left(\frac{2r}{a} - \frac{2\pi N}{3}r^3\right) dr. \quad (2)$$

This integral is easy to evaluate, taking into account that the integrand has a sharp maximum at $r = r_m \equiv 1/\sqrt{\pi Na}$. Consequently one obtains for the current density $j = n_e v$

$$j_{F \rightarrow \infty, n_e \rightarrow 0} \simeq \frac{n_e R}{\bar{\tau}} \simeq n_e (a^3 R)^{1/4} \exp\left(-\frac{4}{3\sqrt{\pi}} \left(\frac{R}{a}\right)^{\frac{3}{2}}\right). \quad (3)$$

Therefore, one can conclude that in the limit $F \rightarrow \infty, n_e \rightarrow 0$ the current is determined by hemispherical traps (Fig. 1a) with an “optimal” radius $r_m = 1/\sqrt{\pi Na}$.

In the case of finite electric fields, a hemispherical trap is not an efficient one, because an electron has a possibility to move in the energetically unfavored directions, and thus to escape the trap (for example, along the dotted arrows in Fig. 1(a)). According to Nguyen and Shklovskii,¹⁵ an “optimal” trap for an electron in large though finite electric fields F consists of a hemisphere to the right and of a cone to the left of the site on which an electron is captured, with a chain of sites along the X axis that provides an easy path into the trap (Fig. 1b). The height h of the cone is chosen so that it is equally hard to escape the trap in all directions taking the chain along the X axes into account: $h = 2rkT/Fa$. Therefore, the smaller is the field, the larger is the volume of a trap with the same dwell time, and consequently the smaller is the probability $p(r)$ of finding such a trap. It means that the average dwell time $\bar{\tau} = \int_0^\infty \tau(r)p(r)dr$ decreases with decreasing field strength, and concomitantly the current density $j \simeq n_e R/\bar{\tau}$ increases with decreasing field. This is the essence of the physical mechanism that causes the NDC effect.¹⁵ To obtain an expression for the current density, one can substitute the volume of the trap shown in Fig. 1b, $V_{\text{trap}} = (1 + kT/Fa)2\pi r^3/3$, instead of the hemispherical trap volume, $2\pi r^3/3$, into the integral (2). The result reads

$$j_{n_e \rightarrow 0} \simeq n_e (a^3 R)^{1/4} \exp\left[-\frac{4}{3\sqrt{\pi}} \left(\frac{R}{a}\right)^{\frac{3}{2}} \left(1 + \frac{kT}{Fa}\right)^{-\frac{1}{2}}\right]. \quad (4)$$

This is the mathematical expression for the NDC. The approach leading to this expression is applicable only for fields $F \gg kT/R$. In smaller fields, the assumption that almost every jump is directed along the axis X is vio-

lated. Therefore one should expect that Eq. (4) overestimates the current density for $F \simeq kT/R$.

Equations (3) and (4) are valid only if the concentration of electrons n_e is small as compared to the concentration of “optimal” traps, $n_m = N \exp[-NV_{\text{trap}}(r_m)]$. In the opposite case, $n_m \ll n_e \ll N$, the “optimal” traps are almost always occupied and play a negligible role. In such a case the most important traps, which determine the drift velocity of electrons, are the ones whose concentration is equal to n_e . One can estimate the electron drift velocity as $v = 1/\tau(r_n)n_e S$, where r_n is a radius of the most important traps, $\tau(r_n)$ is their dwell time, S is their capture crosssection. Assuming $S \simeq R^2 \equiv N^{-2/3}$, one obtains for the current flow $j = n_e v \simeq N^{2/3} \tau(r_n)^{-1}$. For an infinitely large field, the radius r_n is defined via

$$n_e = N \exp(-NV_{\text{trap}}(r_n)) \equiv N \exp\left(-\frac{2\pi N}{3}r_n^3\right),$$

that gives $r_n = R \left(\frac{3}{2\pi} \log \frac{N}{n_e}\right)^{1/3}$. Consequently, the current density is¹⁵

$$j_{F \rightarrow \infty, \substack{n_m \ll n_e \ll 1}} \simeq \frac{N^{2/3}}{\tau(r_n)} \simeq N^{\frac{2}{3}} \exp\left[-\frac{2}{a} \left(\frac{3}{2\pi} \log \frac{N}{n_e}\right)^{\frac{1}{3}}\right]. \quad (5)$$

The corresponding expression for the concentration range $n_m \ll n_e \ll N$ in the case of finite electric fields was also obtained by Nguyen and Shklovskii [see Eq. (11) in Ref. 15].

The case of almost filled sites, $n_e \approx N$, is similar to the case of almost empty sites, $n_e \approx 0$ due to electron-hole symmetry. The current density is a symmetrical function of the electron concentration: $j(n_e) = j(N - n_e)$.

Nguyen and Shklovskii¹⁵ also emphasized that a special consideration is needed for the case of half-filled system, $n_e = N/2$. They have shown that the concept of directed percolation can be used to obtain the current density at infinitely high electric fields. In the half-filled system the trapping of electrons does not play any role, because (due to the electron-hole symmetry) it does not change the electron concentration on the infinite cluster which is responsible for the current. Current is determined by electron jumps to distances $d \in [r_c^d, r_c^d + a/2]$, where r_c^d is the percolation threshold of a directed percolation problem. The number of pairs of sites with distances $d \in [r_c^d, r_c^d + a/2]$ in the infinite cluster per unit area is $1/L_\perp^2$, where $L_\perp = R(2r_c^d/a)^{\nu_\perp}$ is a transversal correlation length of the percolation cluster, and ν_\perp is a critical index.¹⁵ The current density is equal to¹⁵

$$j_{F \rightarrow \infty, \substack{n_e = 1/2}} \simeq \frac{1}{L_\perp^2 \tau(r_c^d)} = N^{\frac{2}{3}} \left(\frac{a}{2r_c^d}\right)^{2\nu_\perp} \exp\left(-\frac{2r_c^d}{a}\right). \quad (6)$$

Nguyen and Shklovskii¹⁵ have also obtained the value of the percolation threshold $r_c^d = (0.93 \pm 0.01) R$ and that of the correlation length index $\nu = 1.2 \pm 0.1$.

The above arguments of Nguyen and Shklovskii¹⁵ provide an analytical theory of non-Ohmic hopping conduction, based on the concept of the trapping-determined transport. The theory is valid for the case of large electric fields in two concentration ranges: $n_e \ll n_m$ and $n_m \ll n_e \ll N$. Most remarkably, this theory predicts the effect of the NDC. Also a theory for the case of the half-filled system ($n_e = N/2$) for infinitely high electric fields ($F \rightarrow \infty$) has been suggested based on the directed percolation-approach.¹⁵

Below we present our numerical study of the field-dependent hopping conductivity. It shows the range of validity for the analytical theory of Nguyen and Shklovskii.¹⁵ Furthermore, the analytical theory is developed below in order to improve the agreement between the analytical and numerical results.

III. MONTE CARLO SIMULATIONS FOR INFINITELY HIGH FIELDS

In order to calculate the electron drift velocity and the current density at high fields, we used a Monte Carlo approach. In the limit of infinitely high fields the direction of the electron motion is prescribed. Therefore it was possible to simulate by a Monte Carlo algorithm the motion of an electron in an infinite medium along the field direction and therefore to avoid any size effects. Without loosing generality one can restrict the maximal length of electron transitions involved into the algorithm by a reasonably large value d_{\max} . In order to simulate the k -th Monte Carlo step in the electron motion, one has to store information only about sites inside a layer $x_k < x < x_k + d_{\max}$, where x_k is the electron coordinate before the k -th step. We have chosen $d_{\max} = 3R$, which provides a possibility to hop to $2\pi d_{\max}^3 N/3 \simeq 57$ neighbors in average. For all sets of parameters used in the simulation the size of the optimal trap r_m considered by Nguyen and Shklovskii was essentially less than d_{\max} . Therefore, the restriction imposed by d_{\max} did not lead to any loss of generality. Before making the next step, the computer can forget all the information about sites in the layer $x_k < x < x_{k+1}$, but it has to get information about new sites in a layer $x_k + d_{\max} < x < x_{k+1} + d_{\max}$. As these “new” sites did not affect the calculation at all previous steps, they can be created at random. Therefore, each Monte Carlo step includes not only the choice of a jump, but also a generation of some “new” sites and deleting some “old” sites. To make their number finite, one should restrict the system size in the directions perpendicular to the field, i.e. in the plane YZ . A calculation domain $0 < y < 120R$, $0 < z < 120R$ with periodical boundary conditions in the plane YZ was used. The motion of a single electron was simulated within the described algorithm in order to evaluate the drift velocity in the limit $n_e \rightarrow 0$.

For finite electron concentrations, we perform simulations in a cubic domain with size $60R \times 60R \times 60R$

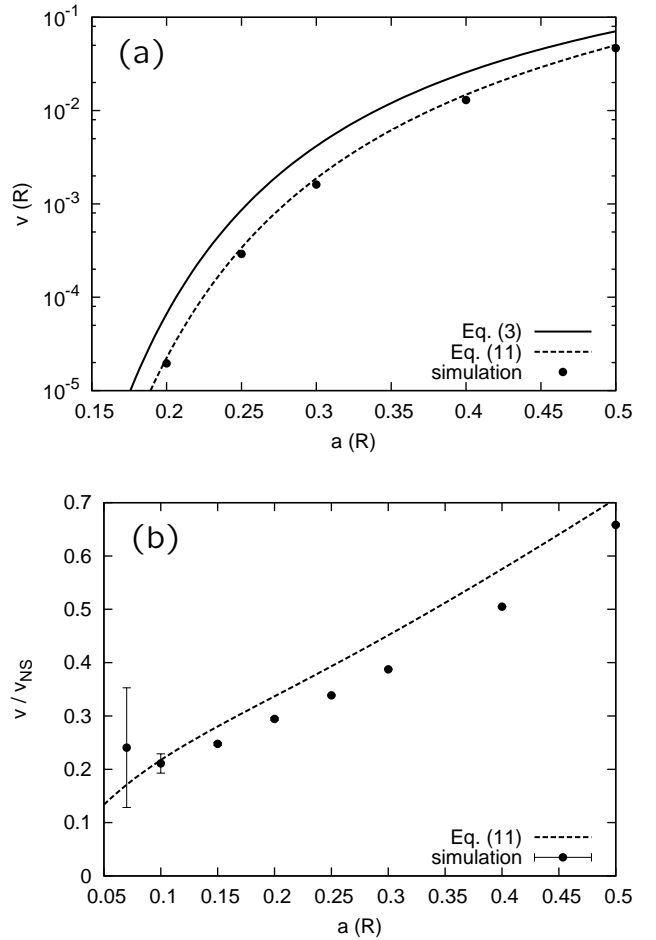


FIG. 2: (a) Drift velocity v in the limit of infinitely large electric field and small electron concentration, as a function of localization length a ; (b) the same data divided by the velocity value predicted in Ref. 15 (Eq. (3)).

and with periodic boundary conditions for all three axes. The rates of all possible jumps are calculated before starting the Monte Carlo steps, but without the factor $n_i(1 - n_j)$ related to occupation. This factor determines which jumps are allowed and which are forbidden. Information about allowed and forbidden jumps is updated at each step. We used a binary-tree data structure for storing the jump rates that gives the possibility to “switch on” and “off” jumps efficiently.

A routine Monte Carlo procedure has been used. In each Monte Carlo step the final site for electron hops was calculated via the probabilities proportional to the hopping rates to different sites and the time Δt spent to jump was calculated via the reciprocal of the sum of rates of all possible jumps. Hops from an occupied site were possible to any empty one in the direction of increasing coordinate x with the restriction that the hop distance is less than $d_{\max} \equiv 3R$. At each hopping event the increment Δx in electron x -coordinate is calculated. An outcome of the simulation is either an average velocity of

an electron,

$$v = \sum \Delta x / \sum \Delta t,$$

in the case of single electron hopping, or a flow of electrons,

$$j = \frac{1}{\Omega} \sum \Delta x / \sum \Delta t,$$

in the case of finite electron concentrations (where Ω is the volume of the calculation domain). The summation was carried out over all sequential Monte Carlo steps. For simulations of the behavior of a single electron in an empty system, 10^7 Monte Carlo steps were used for $a \geq 0.2R$, 10^8 steps for $a = 0.10R$ and $0.15R$ and 10^9 steps for $a = 0.07R$. As a result, for $a \geq 0.15R$ convergence was not worse than 1%.

For finite electron concentration, $5 \cdot 10^7$ Monte Carlo steps were used, this gave a convergence not worse than 1% for a given realization. At $a \leq 0.1R$, there were sometimes essential differences between current densities in different realizations. The scatter is shown by error bars in the figures.

Simulation results for the electron drift velocity $v = j/n_e$ in the limit $n_e \rightarrow 0$ are shown in Fig. 2(a) by dots as a function of the localization length. The analytical result of Nguyen and Shklovskii (Eq. (3)) is shown by the solid line. One can see that Eq. (3) correctly describes the dependence of the drift velocity on the localization length and, furthermore, it correctly estimates the magnitude of the velocity. The concept of Nguyen and Shklovskii on the hopping drift velocity controlled by hemispherical traps is herewith confirmed. However, there is some deviation of the simulation data from the analytical results. To make this deviation more transparent, we plot the ratio of the simulated drift velocity to its analytical prediction (Eq. (3)) in Fig. 2(b). It is seen that Eq. (3) overestimates the electron velocity by a factor of two to five. In Section IVA, some reasons for this mismatch will be considered. The analytical theory is further developed there to give a better agreement with the simulation data. The result of the improved theory for the drift velocity (Eq. (11)) is also shown in Fig. 2 by the dashed line.

The dependence of the current density on the electron concentration is shown in Figs. 3 and 4. Fig. 3 shows this dependence in a wide concentration range, in comparison with the analytical results for small ($n_e \ll n_m$, Eq. (3), solid line) and intermediate ($n_m \ll n_e \ll N$, Eq. (5), dashed line) concentrations. One can see that the simulated concentration dependence can be roughly divided into three parts: for very low concentrations ($n_e < n_m$) the dependence is linear,³⁷ in accordance with Eq. (3); then, for $n_m < n_e < 0.03N$, it becomes superlinear, as described by Eq. (5); and finally, for $n_e > 0.03N$, this dependence is sublinear and is not described by the theory based on the transport controlled by traps. In Section IVB, we will present an analytical approach valid for

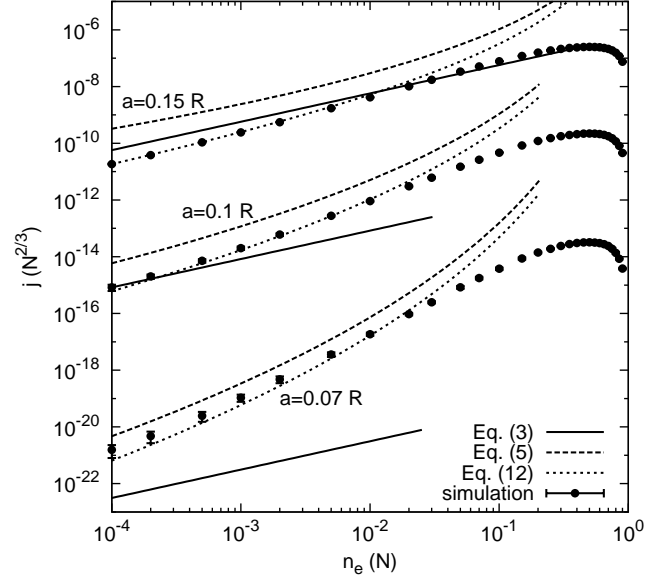


FIG. 3: Current density j as a function of electron concentration n_e for values of the localization length $0.2R$, $0.1R$, and $0.07R$ (from top to bottom). The electric field is infinitely large.

the range of parameters covering the ranges of applicability of Eqs. (3) and (5). The result of this developed approach is Eq. (12) shown by dashed lines in Fig. 3.³⁸ One can see that it provides an accurate description of the current density for any concentration less than $0.03N$.

For $n_e > 0.03N$, the simulated values of the current density are smaller than those predicted by the analytical theory due to the following reason. At sufficiently large electron concentrations, the conducting paths are not almost empty, as is assumed in the theory. Moreover, there are “bottlenecks” for the current, where the electron concentration is much larger than the mean concentration n_e . In these places, the factor of $(1 - n_j)$ in Eq. (1) turns out to be important, and due to this factor the current density is suppressed.

In Fig. 4, the simulation results are shown for the whole range of carrier concentrations. For convenience, all values of current density are divided by the maximum value for the given localization length. For large localization lengths ($a \geq 0.15R$), the concentration dependence of the current density j obeys approximately a parabolic law: $j(n_e) \sim n_e(N - n_e)$ at concentrations in the vicinity of the half filling. One can interpret this behavior in terms of the hopping rates, namely, by substituting the mean occupancy n_e/N instead of n_i and n_j into Eq. (1). Concomitantly, one obtains that the contribution of each pair of sites is proportional to $n_e(N - n_e)$. The same concentration dependence is expected then for the current density.

Fig. 5 shows the simulated dependence of the current density on the localization length (dots) in comparison

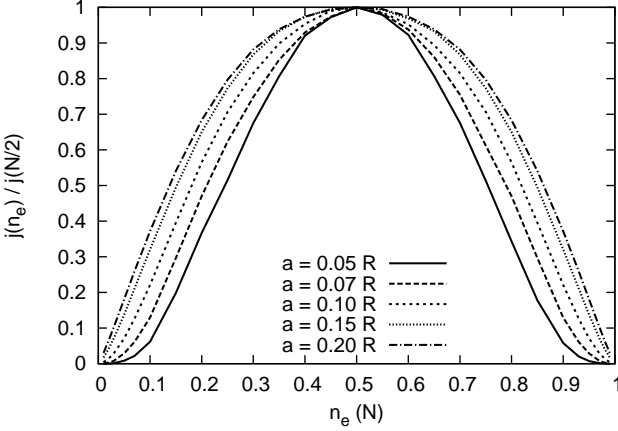


FIG. 4: Current density j as a function of electron concentration n_e , normalized on its maximum value $j(N/2)$, at different localization lengths. The electric field is infinitely large.

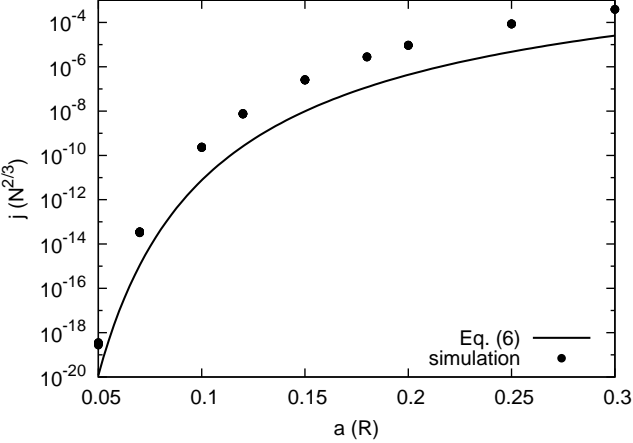


FIG. 5: Current density j as a function of localization length a for the half-filled system ($n_e = N/2$). The electric field is infinitely large.

with the analytical theory based on the concept of directed percolation (Eq. (6), solid line) for $n_e = N/2$. Apparently, the theory of Nguyen and Shklovskii¹⁵ correctly describes this dependence within the range of current densities of almost 15 orders of magnitude. However, the theory underestimates the magnitude of the current density by approximately a factor of 30. Further research is necessary to clarify the reasons of this discrepancy.

IV. ANALYTICAL THEORY FOR INFINITELY HIGH FIELDS

Our numerical studies show that although the analytical description of hopping conduction in very strong electric field by Nguyen and Shklovskii is qualitatively correct the quantitative predictions differ sometimes by

more than an order of magnitude from the numerical results. In this Section, we show how to improve the accuracy of the analytical theory.

A. Limit of $n_e \rightarrow 0$

For low electron concentrations $n_e \ll n_m$, where $n_m = N \exp[-\frac{2\pi}{3}(R/\pi a)^{3/2}]$ is the concentration of the “optimal” traps, the prediction of Ref. 15 for the electron drift velocity is expressed by Eq. (3). Now we discuss several corrections to this equation.

1) There is a numeric factor of $(4\pi)^{1/4} \approx 1.88$ in $\bar{\tau}$, arising from the evaluation of the integral (2) that should be taken into account. It gives a factor of $(4\pi)^{-1/4}$ for the drift velocity.

2) The mean electron displacement along the X axis, $\langle \Delta x \rangle$, is taken equal to R in Ref. 15. We performed Monte Carlo calculations for $\langle \Delta x \rangle$ as a function of the localization length a and get the following fitting expression:

$$\langle \Delta x \rangle = R (0.385 + 0.45a^2/R^2) \quad (7)$$

(the accuracy of fitting is not worse than 0.3 % in the range $0.05 \leq a/R \leq 0.2$). Therefore, the drift velocity $v = \langle \Delta x \rangle / \bar{\tau}$ gets an additional factor equal approximately to 0.5.

3) The dwell time $\tau(r)$ of a trap with a radius r is in fact somewhat less than the value $\exp(2r/a)$ used in Ref. 15 because an electron can escape the trap by moving not only to the nearest site to the right, but also to a more distant site. A contribution Γ_1 of these distant sites to the escaping rate is

$$\Gamma_1 = \int_r^\infty e^{-2r_1/a} 2\pi N r_1^2 dr_1 = e^{-2r/a} \pi N a \left(r^2 + ar + \frac{a^2}{2} \right).$$

Then, the dwell time $\tau(r)$ is a reciprocal of the sum $\Gamma_0 + \Gamma_1$, where $\Gamma_0 = \exp(-2r/a)$ is the rate of a jump to the nearest neighbor:

$$\tau(r) = \frac{1}{\Gamma_0 + \Gamma_1} = \frac{\exp(2r/a)}{1 + \pi N a (r^2 + ar + a^2/2)}. \quad (8)$$

For $r = r_m \equiv (\pi N a)^{-1/2}$, $\tau(r)$ is approximately half of $\exp(2r/a)$, that results in a factor of two in the drift velocity.

4) The geometrical crosssections of larger traps have larger capture crosssections for electrons than the smaller ones. This results in different probabilities for carriers to be captured by traps with different radii. The probability $\tilde{p}(r)dr$ that the next visited site will be a trap with radius in the range $(r, r + dr)$ is

$$\tilde{p}(r)dr = \frac{S(r)}{\langle S \rangle} p(r)dr,$$

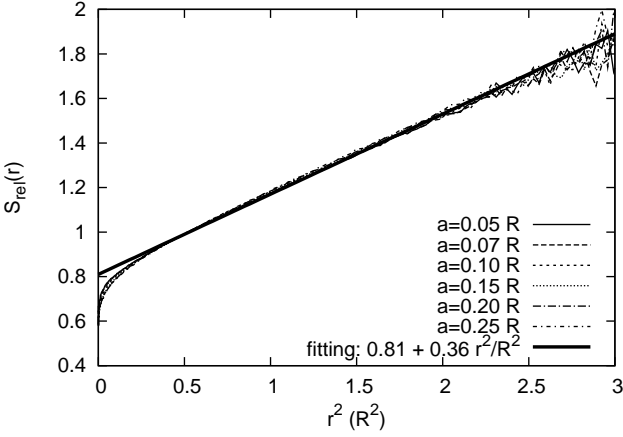


FIG. 6: Relative capture crosssection as a function of squared trap radius.

where $p(r) = 2\pi N r^2 \exp(-2\pi N r^3/3)$, $S(r)$ is a capture crosssection of a trap with radius r , and $\langle S \rangle = \int S(r)p(r)dr$ is a mean crosssection. Below we will use a notation $S_{\text{rel}}(r)$ for a “relative crosssection” $S(r)/\langle S \rangle$. Then, instead of Eq. (2) we get

$$\bar{\tau} = \int_0^\infty \tau(r) S_{\text{rel}}(r) p(r) dr. \quad (9)$$

We calculated the relative crosssections with Monte Carlo method as ratios $N_{tr}[r, r+\Delta r]/(N_j p(r)\Delta r)$, where $N_{tr}[r, r+\Delta r]$ is a number of traps with radii in the specified range visited by an electron, and N_j is a total number of electron jumps. We used $N_j = 10^8$ and $\Delta r = 0.01R$. The results are presented in Fig. 6. The relative crosssection is almost independent of the localization length for $r > 0.3R$. Its dependence on the trap radius is described by the quadratic function:

$$S_{\text{rel}}(r) = 0.81 + 0.36 r^2/R^2. \quad (10)$$

For the “optimal” traps with $r = r_m \equiv (\pi N a)^{-1/2}$ we get $S_{\text{rel}}(r_m) \sim a^{-1}$ in the limit $a \rightarrow 0$. According to Eq. (9), it results in a factor of $\sim a^{-1}$ for the mean dwell time $\bar{\tau}$ and, consequently, in a factor of $\sim a$ for the drift velocity.

Now we can improve Eq. (3) of Nguyen and Shklovskii, starting from Eq. (9). Since the integrand has a sharp maximum at $r_m = (\pi N a)^{-1/2}$, we can estimate the integral approximately as

$$\bar{\tau} \approx \tau(r_m) S_{\text{rel}}(r_m) p(r_m) (\pi R^3 a/4)^{1/4} N^{-1}.$$

Then, using Eqs. (7), (8), and (10), we get the following expression for the drift velocity $v = \langle \Delta x \rangle / \bar{\tau}$:

$$v \approx \frac{(0.85 + 0.45 \frac{a^2}{R^2}) \left[1 + \pi N a \left(\frac{1}{\pi N a} + \sqrt{\frac{a}{\pi N}} + \frac{a^2}{2} \right) \right]}{(4\pi)^{1/4} (0.81 + 0.36 \frac{R}{\pi a})} v_{\text{NS}}.$$

Here $v_{\text{NS}} = j/n_e$ is the drift velocity corresponding to Eq. (3). Finally, the latter expression can be fitted (with accuracy of about 3 % for $a \leq 0.2R$) by a simple formula,

$$v \approx \frac{a}{R} \left(1.4 + 2.1 e^{-10 a/R} \right) v_{\text{NS}}. \quad (11)$$

This expression is to be considered as a corrected analytical form for the drift velocity at infinitely high fields in the limit of small electron concentration.

A comparison of Eq. (11) with the values of the drift velocity obtained by the Monte Carlo method is shown in Fig. 2. The difference between the analytical and simulated results does not exceed 20 %. We believe that the main source of this small difference is some inaccuracy in determining $\tau(r)$ by Eq. (8). In fact, for a given trap radius there is some distribution of the dwell times. The quantity $\tau(r)$ contributing to Eq. (9) is the mean dwell time for radius r . However, Eq. (8) gives the reciprocal value of the mean escaping rate that is slightly smaller than $\tau(r)$. For this reason, Eq. (11) can slightly overestimate the drift velocity.

B. Finite electron concentration

Let us now try to improve the analytical approach at finite, though small electron concentration, $n_e \ll N/2$. In this case, electron flow can be considered as a homogeneous one on the scale of distances between the traps that determine the transport. Hence one can express the frequency ν_{in} of electron capture by a trap as $\nu_{in} = j S (1 - \bar{n})$, where j is the current density, S is the trap capture crosssection, and \bar{n} is its mean occupancy. Under the steady-state conditions, $\nu_{in} = \nu_{out}$, where $\nu_{out} = \bar{n}/\tau$ is a frequency of emission of electrons from the trap, τ is a dwell time. From this equation one can get \bar{n} :

$$\bar{n} = \frac{1}{1 + (j S \tau)^{-1}}.$$

Since in a snapshot of the system almost all electrons are captured by traps, the total electron concentration n_e is

$$n_e = \int_0^\infty \bar{n}(r) p(r) dr = \int_0^\infty \frac{p(r) dr}{1 + (j S(r) \tau(r))^{-1}}. \quad (12)$$

The dwell time $\tau(r)$ can be estimated by Eq. (8). In order to find the crosssection $S(r)$, one should note that the mean crosssection $\langle S \rangle$ is equal to $1/N \langle \Delta x \rangle$. Consequently,

$$S(r) = \frac{S_{\text{rel}}(r)}{N \langle \Delta x \rangle} = R^2 \frac{0.81 R^2 + 0.36 r^2}{0.385 R^2 + 0.45 a^2}. \quad (13)$$

Equation (12) with $\tau(r)$ and $S(r)$ determined by Eqs. (8) and (13), respectively, gives a functional dependence between the electron concentration and the current

density for any $n_e \ll N/2$. Fig. 3 evidences a good agreement between Eq. (12) and the Monte Carlo calculations for $n_e \leq 0.03 N$.

Although there is probably no simple way to resolve Eq. (12) with respect to j analytically in the general case, it is possible to simplify this equation in some limiting cases. For small n_e and j ($n_e \ll n_m$), the unity term in the denominator of Eq. (12) can be dropped, and we get $n_e = j/v$, where the drift velocity $v = \langle \Delta x \rangle / \bar{\tau}$ is determined by Eq. (11). In the opposite limit ($n_e \gg n_m$), one can evaluate Eq. (12) as

$$n_e \approx \int_{r_n}^{\infty} p(r) dr = N \exp \left(-\frac{2\pi N r_n^3}{3} \right),$$

where a cutting parameter r_n is given by condition $jS(r_n)\tau(r_n) = 1$. Therefore,

$$j = \frac{1}{S(r_n)\tau(r_n)} \quad (14)$$

with

$$r_n = R \left(\frac{3}{2\pi} \log \frac{N}{n_e} \right)^{1/3}. \quad (15)$$

Equation (14), with parameters determined by Eqs. (8), (13) and (15) is the improved version of Eq. (5) by Nguyen and Shklovskii for the concentration range $n_m \ll n_e \ll N/2$.

V. HOPPING TRANSPORT AT FINITE ELECTRIC FIELDS

So far we have considered the limiting case of infinitely high electric fields. Let us now turn to the field dependence of the charge carriers velocity in order to reveal the possibility of the negative differential conductivity predicted by Nguyen and Shklovskii.¹⁵ Eq. (4) predicts a decreasing drift velocity with increasing electric field, provided the field is strong enough. On the other hand, for very small fields, Ohmic transport can be expected, i.e., the drift velocity should depend linearly on the field. In order to simulate hopping transport at finite electric fields, we solved a system of balance equations instead of using a direct MC simulation. In the following subsection A we describe the details of the numerical procedure, while the results are presented in subsection B.

A. Balance equation method

We consider a cubic system (side length L) with randomly placed sites. Periodic boundary conditions are used in all directions. The balance equation for the occupation probability p_i of a site i has the form^{29,30,31,32,33,34}

$$\sum_{j \neq i} p_i \Gamma_{ij} (1 - p_j) = \sum_{j \neq i} p_j \Gamma_{ji} (1 - p_i). \quad (16)$$

If all occupation probabilities p_i are small, i.e. the charge carrier concentration is low, the balance equation can be linearized:

$$\sum_{j \neq i} p_i \Gamma_{ij} = \sum_{j \neq i} p_j \Gamma_{ji}. \quad (17)$$

These equations are solved by defining

$$\mathbf{p} = \begin{pmatrix} p_1 \\ p_2 \\ p_3 \\ \vdots \end{pmatrix} \text{ and } \mathbf{M} = \begin{pmatrix} -\Gamma_1 & \Gamma_{21} & \Gamma_{31} & \cdots \\ \Gamma_{12} & -\Gamma_2 & \Gamma_{32} & \cdots \\ \Gamma_{13} & \Gamma_{23} & -\Gamma_3 & \cdots \\ \vdots & \vdots & \vdots & \ddots \end{pmatrix}, \quad (18)$$

where $\Gamma_i = \sum_{j \neq i} \Gamma_{ij}$ is the rate of jumping out of site i . The equation is then $\mathbf{M}\mathbf{p} = 0$, which we solve numerically. The matrix \mathbf{M} defined in this way is singular, which makes a direct solution rather difficult. By replacing one of the balance equations with the normalization

$$\sum_i p_i = 1, \quad (19)$$

the matrix becomes nonsingular, and the solution can be obtained more efficiently. Additionally, the solution obtained in this way is correctly normalized. After this replacement, the equation has the form:

$$\begin{pmatrix} 1 & 1 & 1 & \cdots \\ \Gamma_{12} & -\Gamma_2 & \Gamma_{32} & \cdots \\ \Gamma_{13} & \Gamma_{23} & -\Gamma_3 & \cdots \\ \vdots & \vdots & \vdots & \ddots \end{pmatrix} \begin{pmatrix} p_1 \\ p_2 \\ p_3 \\ \vdots \end{pmatrix} = \begin{pmatrix} 1 \\ 0 \\ 0 \\ \vdots \end{pmatrix} \quad (20)$$

As in Section III, the rates for jumps longer than d_{\max} are assumed to be zero. Hence, it is efficient to use a sparse storage scheme for the matrix, where only the non-zero elements are stored. We obtained the most accurate results in the shortest time by solving the equation by LU factorization (in Matlab or Octave with the \ operator). This method demands much memory, and did not work for L above about $22 R$ on a 32-bit computer.

When the steady-state occupation probabilities are known, the average velocity of a charge carrier along the field direction is given by

$$\langle v_x \rangle = \sum_{i,j \neq i} p_i \Gamma_{ij} (x_j - x_i), \quad (21)$$

and the mobility is then $\mu = \frac{\langle v_x \rangle}{F}$.

B. Field dependence of the current density

The simulated dependence of the drift velocity v on the electric field F is presented in Fig. 7. Simulations are performed for 20^3 sites in a cubic domain with the size $L = 20 R$, in the limit of infinitely small electron concentration. Different symbols refer to different localization

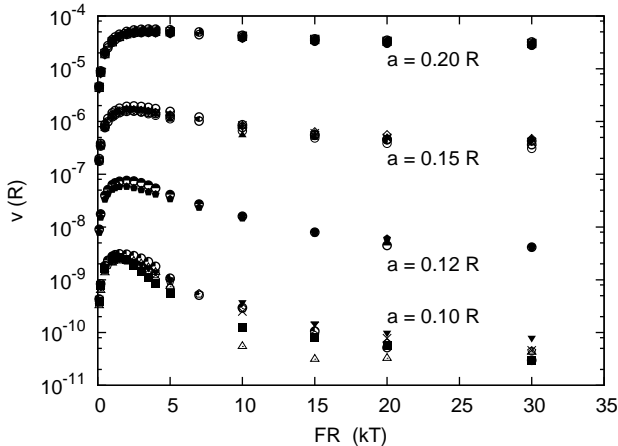


FIG. 7: Drift velocity as a function of the electric field, for different localization lengths. The system size L is $20 R$.

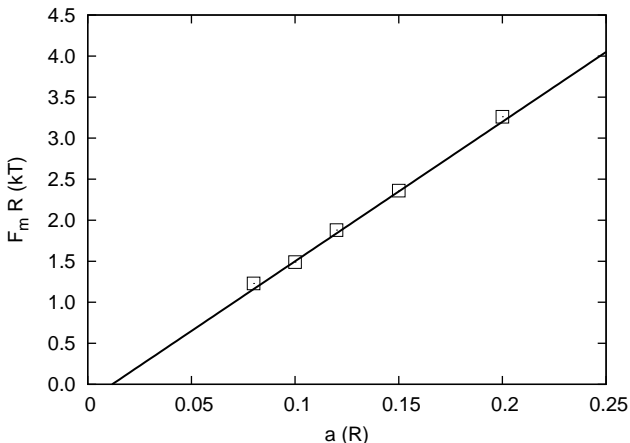


FIG. 8: The field F_m corresponding to the maximum of the drift velocity as a function of the localization length a . The linear fit is given by $F_m R / kT = 17a / R - 0.2$.

lengths and/or different realizations of the distribution of sites in the domain. The size of the simulated system was 10 times larger than that in the simulations of Levin et al.,²¹ whose computer simulations for the first time confirmed the existence of the NDC effect for hopping transport.

In the limit of small electric field, $FR/kT \ll 1$, simulations show an Ohmic conductivity, i.e., v is proportional to F , in accordance to the Miller–Abrahams concept of the resistance network.^{20,35} With increasing field, the drift velocity reaches a maximum value. The field strength F_m corresponding to the maximum of the velocity appears to be nearly proportional to the localization length a within the range $0.08 R < a < 0.2 R$ (see Fig. 8). At field strengths $F > F_m$ the NDC appears, i. e. the drift velocity drops with increasing field. Simulations show the presence of the NDC for localization lengths up to $0.3 R$; when the localization length is decreased, the

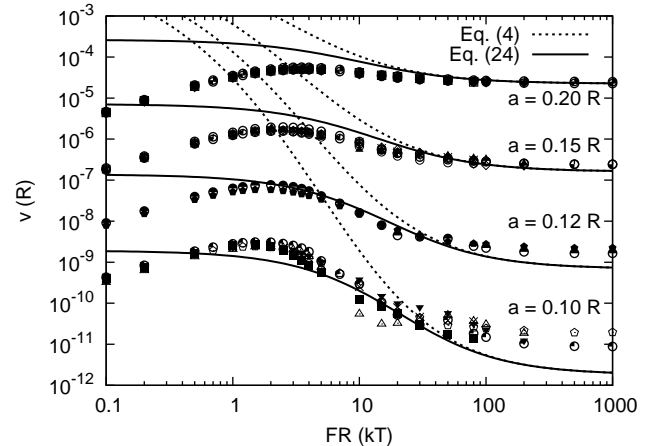


FIG. 9: Drift velocity as a function of the electric field for different localization lengths. The curves show Eq. (4) and Eq. (24), scaled to approach Eq. (11) in the limit of large fields. The system size L is $20 R$.

NDC effect becomes more pronounced.

Fig. 9 shows the comparison between the simulation results (symbols) and the predictions of Nguyen and Shklovskii¹⁵ (Eq. (4), dashed lines). For better agreement between the theory and the simulation at $F \rightarrow \infty$, we take into account the F -independent correction (11) to Eq. (4). Some discrepancies between the simulated and predicted drift velocities remain at large fields for $a = 0.10 R$ and $a = 0.12 R$. We believe that these discrepancies are due to the small size of the simulated system. In fact, the simulated system must be large enough to contain a reasonable number of optimal traps. The concentration of optimal traps decreases sharply with decreasing localization length, so that at smaller localization lengths larger systems are needed. Thus, for small localization length ($0.10 R$ and $0.15 R$), only the shape of the simulated field dependence should be taken as representative, but not the values of the calculated velocities themselves.

The range of applicability of Eq. (4) is determined by the condition $FR/kT \gg 1$. One can see nevertheless that even within this range the field dependence of the velocity is much weaker than the one predicted by Eq. (4). This result forced us to consider another possible optimal trap shape for the case of a finite field as compared to the one considered in Ref. 15.

The essential feature of the optimal trap proposed by Nguyen and Shklovskii (Fig. 1b) is the chain of sites along the axis of the cone. This chain was introduced in order to provide an easy path for an electron into a trap. The chain affects the trap shape and volume, as it serves also as a channel for escaping of an electron from the trap. We suggest that at moderate localization lengths ($a \simeq 0.1 R$) traps without such a chain can also play a significant role. Our next aim is to consider the shape of traps without a chain of sites and to estimate their influence on the electron conduction.

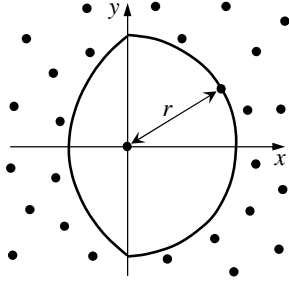


FIG. 10: Geometry of the optimal trap at finite electric fields without a chain of sites leading into the trap.

A sketch of such a trap is shown in Fig. 10. Its shape is defined by the condition that the rate of jumping from the central site to any point of the trap's surface is the same. From Eq. (1) one can see that in the positive direction along the axis X the trap is bounded by a hemisphere, and in the negative direction—by a surface defined by an equation

$$\frac{F}{kT} x - \frac{2}{a} \sqrt{x^2 + y^2 + z^2} = -\frac{2r}{a}, \quad (22)$$

where r is the radius of the hemisphere, and the origin is placed at the central site of the trap. The surface determined by Eq. (22) is a quadric surface (an ellipsoid, a paraboloid, or a hyperboloid, depending on the values of parameters). The volume of the trap, V'_{trap} is

$$V'_{\text{trap}}(r) = \frac{2\pi r^3}{3} \left(1 + \frac{c+2}{2(c+1)^2} \right), \quad (23)$$

where $c \equiv Fa/2kT$.

To obtain the drift velocity v (or the current density $j = n_e v$) in the assumption that the most important traps are those shown in Fig. 10, one can proceed in the same way as the one applied in Section II to get Eq. (4); the only difference is using $V'_{\text{trap}}(r)$ instead of Nguyen and Shklovskii's trap volume $V_{\text{trap}}(r) = \frac{2\pi r^3}{3} (1 + \frac{kT}{Fa})$. The result is

$$j_{n_e \rightarrow 0} \simeq n_e (a^3 R)^{\frac{1}{4}} \exp \left[-\frac{4}{3\sqrt{\pi}} \left(\frac{R}{a} \right)^{\frac{3}{2}} \left(1 + \frac{c+2}{2(c+1)^2} \right)^{-\frac{1}{2}} \right]. \quad (24)$$

For the optimal trap radius one gets

$$r_m = \frac{1}{\sqrt{\pi Na}} \left(1 + \frac{c+2}{2(c+1)^2} \right)^{-1/2}.$$

Since $V'_{\text{trap}}(r) < V_{\text{trap}}(r)$, the new trap shape gives a weaker field dependence of the drift velocity, and a better agreement with the data from simulations, as one can see in Fig. 9. However, the simulated field dependence appears even weaker than the one expressed by Eq. (24). It leads to the assumption that an actual optimal trap has a shape different from both Fig. 1b and Fig. 10, and hence has a different volume.

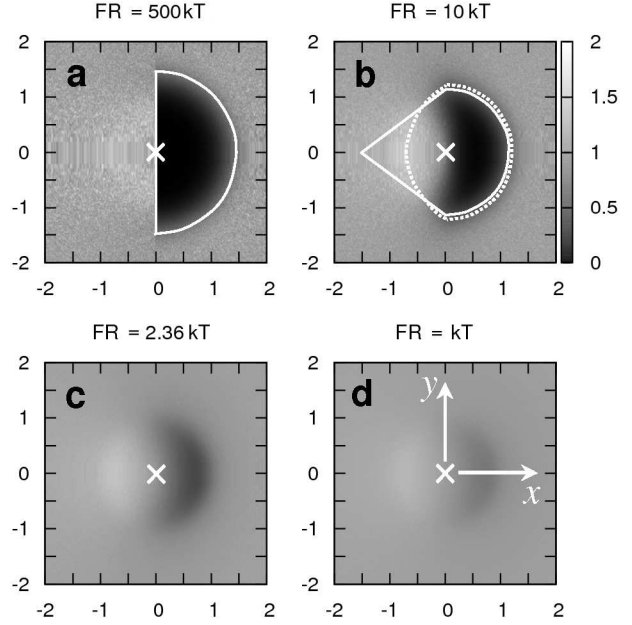


FIG. 11: Time-averaged density of sites around the charge carrier for different fields at the localization length $a = 0.15 R$. The position of a charge carrier (at the origin) is pointed out by a cross. Boundaries of optimal traps predicted in Ref. 15 (see Fig. 1) are depicted by solid lines, the boundary of the trap sketched in Fig. 10 by the dotted line. Spatial coordinates are in units of R . The value $2.36kT$ for FR corresponds to the maximum of the drift velocity.

To further investigate the shape of the most efficient traps, we collect information about the trap shape from the simulations. Fig. 11 show the time-average of the density of sites around the charge carrier. To calculate this density $\rho(\mathbf{r})$, the space was divided into small elements of equal volume ΔV ; then $\rho(\mathbf{r})$ was evaluated as a sum over pairs of sites:

$$\rho(\mathbf{r}) = \frac{1}{\Delta V} \sum_{i \neq j} p_i \chi_{ij}(\mathbf{r}),$$

where p_i is an occupation probability of the i -th site; $\chi_{ij}(\mathbf{r}) = 1$ if the vector $(\mathbf{r}_j - \mathbf{r}_i)$ belongs to the same spatial element as the vector \mathbf{r} ; otherwise $\chi_{ij}(\mathbf{r}) = 0$. Finally, values of $\rho(\mathbf{r})$ were averaged over several realizations of site distributions.

Since the carrier spends the most time in the efficient traps, the density distribution $\rho(\mathbf{r})$ directly reflects the shape of these traps. At high fields (Fig. 11a) the hemispherical shape and the size of the trap are in an excellent agreement with the Nguyen and Shklovskii's theory. However, at moderate fields, in the region of the NDC (Fig. 11(b)), neither Fig. 1(b) nor Fig. 10 describe the simulated optimal trap. The optimal trap consists in such a case of a hemisphere in the spatial region $x > 0$, and of a toroidal "barrier" in the region $x < 0$, adjoining to a periphery of the hemisphere. The volume of the optimal trap turns out to be smaller than the one predicted

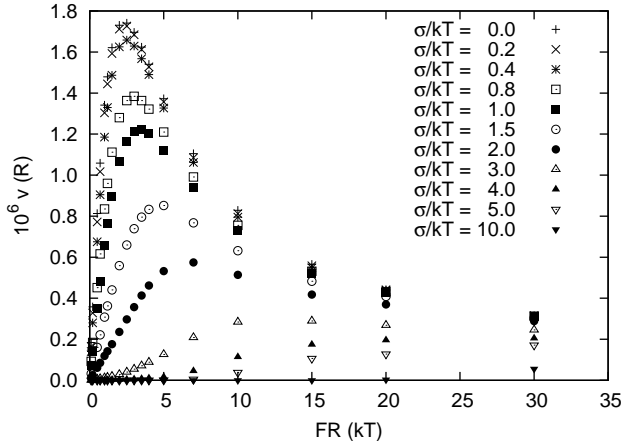


FIG. 12: Drift velocity v versus electric field F for Gaussian disorder in site energies. Disorder is characterized by a standard deviation σ of site energies from the reference energy. The localization length $a = 0.15 R$.

by both Eq. (4) and Eq. (24), in accordance with the result that the simulated NDC effect is weaker than the predicted one. We would like to emphasize that the numerically obtained NDC has exactly the origin predicted by Nguyen and Shklovskii,¹⁵ consisting in spreading of the optimal trap into the region $x < 0$ at finite fields and consequently in the increase of the trap volume with decreasing the field strength. The possibility of traps in the form of clusters instead of single chains of sites has been considered in Ref. 18. We interpret our numerical result as a confirmation of that idea.

A further decrease of the electric field F results in the washing out the empty region in the density of sites $\rho(\mathbf{r})$, as shown in Fig. 11(c) for $F = F_m$. Finally, at small F the trap almost disappeared (Fig. 11(d)), which points to a negligible role of the trapping effect in the regime of Ohmic conduction.

Materials studied experimentally usually have disorder not only in the spatial distribution of localized states, but also in the site energies.^{3,5,36} It is therefore necessary to check how stable the NDC effect is with respect to energetic disorder. In order to study the role of the energetic disorder for the NDC effect, we repeated the simulation in a system with a Gaussian distribution of site energies, characterized by the standard deviation σ . Fig. 12 shows that introducing a random energy for each

site (with a Gaussian distribution) decreases the drift velocity and it also decreases the height of the peak of the velocity as a function of the electric field as compared to systems with only spatial disorder. This weakening of the NDC effect with the increase of the energetic disorder (or with the decrease of temperature) is in agreement with experimental observations.^{18,19} Generally, the NDC effect is confirmed herewith also for systems with the energetic disorder. However, at extremely large energetic disorder (parameter σ), the peak in the field dependence of the drift velocity disappears completely. The effect of energetic disorder becomes smaller at larger fields, as expected from the fact that in the limit $F \rightarrow \infty$ the hopping rates do not depend on site energies.

VI. CONCLUSIONS

Numerical studies of the field-dependent drift velocity of charge carriers in the hopping regime at high electric fields confirm the prediction of the existing analytical theories^{14,15} that the negative differential conductivity is inherent for this transport mode. However, the shape of the field dependence on the current density obtained numerically differs essentially from the one predicted so far.¹⁵ The analytical theory has been improved to give a much better agreement with the numerical results. In the limit of the infinitely high electric fields, the predictions of the analytical theory of Nguyen and Shklovskii¹⁵ are to much extent confirmed by our straightforward Monte Carlo simulations.

Acknowledgments

The authors are indebted to Prof. Boris Shklovskii for numerous valuable comments. Financial support from the Academy of Finland project 116995 and the TEKES NAMU project, from the Deutsche Forschungsgemeinschaft and that of the Fonds der Chemischen Industrie is gratefully acknowledged. A. V. N. thanks the Russian Foundation for Basic Research (project 06-02-16988) and the Dynasty Foundation for financial support. The authors thank Oleg Rubel and Kakhaber Jandieri for stimulating discussions.

* Electronic address: nenashev@isp.nsc.ru

¹ H. Böttger and V. V. Bryksin, *Hopping conduction in solids* (VCH Akademie-Verlag Berlin, 1985).

² S. Baranovski, ed., *Charge Transport in Disordered Solids with Applications in Electronics* (John Wiley & Sons, Ltd, Chichester, 2006).

³ H. Bässler, *Semiconducting Polymers*, G. Hadzioannou and P. F. van Hutter (eds.) (John Wiley & Sons, Inc.,

New York, 2000), p. 365.

⁴ M. Pope and C. E. Swenberg, *Electronic Processes in Organic Crystals and Polymers* (Oxford University Press, Oxford, 1999).

⁵ H. Bässler, *Phys. Status Solidi B* **175**, 15 (1993).

⁶ P. M. Borsenberger, E. H. Magin, M. van der Auweraer, and F. C. de Schryver, *Phys. Status Solidi (a)* **140**, 9 (1993).

⁷ M. van der Auweraer, F. C. de Schryver, P. M. Borsenberger, and H. Bässler, *Advanced Materials* **6**, 199 (1994).

⁸ M. Abkowitz, *Phil. Mag. B* **65**, 817 (1992).

⁹ A. Peled and L. B. Schein, *Chem. Phys. Lett.* **153**, 422 (1988).

¹⁰ L. B. Schein, *Phil. Mag. B* **65**, 795 (1992).

¹¹ P. E. Parris and B. D. Bookout, *Phys. Rev. B* **53**, 629 (1996).

¹² A. Hirao, H. Nishizawa, and M. Sugiuchi, *Phys. Rev. Lett.* **75**, 1787 (1995).

¹³ H. Cordes, S. D. Baranovskii, K. Kohary, P. Thomas, S. Yamasaki, F. Hensel, and J.-H. Wendorff, *Phys. Rev. B* **63**, 094201 (2001).

¹⁴ H. Böttger and V. V. Bryksin, *Phys. Status Solidi B* **96**, 219 (1979).

¹⁵ Nguyen Van Lien and B. I. Shklovskii, *Solid State Commun.* **38**, 99 (1981).

¹⁶ E. I. Levin and B. I. Shklovskii, *Solid State Commun.* **67**, 233 (1988).

¹⁷ D. I. Aladashvili, Z. A. Adamia, K. G. Lavdovskii, E. I. Levin, and B. I. Shklovskii, *Pis'ma v Zh. Eksp. Teor. Fiz.* **47**, 390 (1988), *Sov. Phys. JETP Lett.* **47**, 466 (1988).

¹⁸ D. I. Aladashvili, Z. A. Adamia, K. G. Lavdovskii, E. I. Levin, and B. I. Shklovskii, *Fiz. Tekhn. Poluprov.* **24**, 234 (1990), *Sov. Phys. Semicond.* **24**, 143 (1990).

¹⁹ D. I. Aladashvili, Z. A. Adamia, K. G. Lavdovskii, E. I. Levin, and B. I. Shklovskii, in *Hopping and related phenomena*, edited by H. Fritzsche and M. Pollak (World Scientific, 1990).

²⁰ B. I. Shklovskii and A. L. Efros, *Electronic Properties of Doped Semiconductors* (Springer-Verlag, 1984).

²¹ E. I. Levin, Nguyen Van Lien, and B. I. Shklovskii, *Fiz. Tekhn. Poluprov.* **16**, 815 (1982), *Sov. Phys. Semicond.* **16**, 523 (1982).

²² J. G. Simmons and R. R. Verderber, *Proc. R. Soc. London A* **391**, 77 (1967).

²³ R. E. Thurstans and D. P. Oxley, *J. Phys. D* **35**, 802 (2002).

²⁴ L. D. Bozano, B. W. Kean, V. R. Deline, J. R. Salem, and J. C. Scott, *Appl. Phys. Lett.* **84**, 607 (2004).

²⁵ L. D. Bozano, B. W. Kean, M. Beinhoff, K. R. Carter, P. M. Rice, and J. C. Scott, *Advanced Functional Materials* **15**, 1933 (2005).

²⁶ H. S. Majumdar, J. K. Baral, R. Österbacka, O. Ikkala, and H. Stubb, *Organic Electronics* **6**, 188 (2005).

²⁷ F. Verbakel, S. C. J. Meskers, R. A. J. Janssen, H. L. Gomes, M. Colle, M. Buchel, and D. M. de Leeuw, *Appl. Phys. Lett.* **91**, 192103 (2007).

²⁸ J. K. Baral, H. S. Majumdar, A. Laiho, H. Jiang, E. I. Kauppinen, R. H. A. Ras, J. Ruokolainen, O. Ikkala, and R. Österbacka, *Nanotechnology* **19**, 035203 (2008).

²⁹ Z. G. Yu, D. L. Smith, A. Saxena, R. L. Martin, and A. R. Bishop, *Phys. Rev. Lett.* **84**, 721 (2000).

³⁰ Z. G. Yu, D. L. Smith, A. Saxena, R. L. Martin, and A. R. Bishop, *Phys. Rev. B* **63**, 085202 (2001).

³¹ W. F. Pasveer, J. Cottaar, P. A. Bobbert, and M. A. J. Michels, *Synth. Met.* **152**, 157 (2005).

³² J. Cottaar and P. A. Bobbert, *Phys. Rev. B* **74**, 115204 (2006).

³³ F. Jansson, S. D. Baranovskii, G. Sliaužys, R. Österbacka, and P. Thomas, *Phys. Status Solidi C* **5**, 722 (2008).

³⁴ F. Jansson, S. D. Baranovskii, F. Gebhard, and R. Österbacka, *Phys. Rev. B* **77**, 195211 (2008).

³⁵ A. Miller and E. Abrahams, *Phys. Rev.* **120**, 745 (1960).

³⁶ O. Rubel, S. D. Baranovskii, P. Thomas, and S. Yamasaki, *Phys. Rev. B* **69**, 014206 (2004).

³⁷ This linear part is seen in Fig. 3 only for $a = 0.15R$, because for $a = 0.1R$ and $0.07R$ the value n_m is less than $10^{-4} N$.

³⁸ The integral in Eq. (12) is evaluated numerically.